

# Effects of Phosphorus on Loosely Bound and Tightly Bound Extracellular Polymer Substances in Aerobic Granular Sludge



This work is licensed under a  
Creative Commons Attribution 4.0  
International License

L. L. Yan,<sup>a</sup> L. B. Yu,<sup>a</sup> Q. P. Liu,<sup>a</sup> X. L. Zhang,<sup>a</sup>  
Y. Liu,<sup>a</sup> M. Y. Zhang,<sup>a</sup> S. Liu,<sup>a</sup> Y. Ren,<sup>b</sup> and Z. L. Chen<sup>b,\*</sup>

<sup>a</sup>School of Resource and Environment,  
Northeast Agricultural University, Harbin 150030 China

<sup>b</sup>School of Environment, Harbin Institute of Technology,  
Harbin 150090, China

doi: 10.15255/CABEQ.2018.1445

Original scientific paper  
Received: July 17, 2018  
Accepted: March 4, 2019

The stability of aerobic granular sludge (AGS) is closely related to its extracellular polymeric substances (EPS). In this study, the composition and physicochemical characteristics of EPS in AGS were determined to evaluate their roles in AGS stability. The study evaluated the influence of influent phosphorus concentration on EPS protein (PN), polysaccharide (PS) and orthophosphate content, zeta potential ( $\zeta$ ) and fluorescence spectrum (EEM) in loosely bound EPS (LB-EPS) and tightly bound EPS (TB-EPS). With higher influent phosphorus concentration, the PN, PS and orthophosphate content were higher, as was the zeta potential in TB-EPS, but it had less influence on LB-EPS. Three-dimensional, synchronous fluorescence spectroscopy and fluorescence region integral (FRI) showed that protein-like substances were the primary components of LB-EPS and TB-EPS. Phosphorus had a dynamic quenching effect on EPS at a concentration between 0 mg L<sup>-1</sup> and 17.5 mg L<sup>-1</sup>, which is the indirect production of phosphorus by cations. An increased concentration of influent phosphorus was beneficial to AGS stability.

## Keywords:

aerobic granular sludge, phosphorus, TB-EPS, LB-EPS, fluorescence spectrum

## Introduction

Aerobic granular sludge (AGS) is composed of a multispecies microbial aggregation of self-curing groups with a degree of self-balancing capacity. Compared with traditional activated sludge, AGS has better settling performance, stronger resistance to impact loading, and higher biomass.<sup>1</sup> AGS technology has been recognized as one of the most promising biological wastewater treatment technologies and has become a heavily studied topic in wastewater treatment research. However, it is well-known that, after reaching a certain size, some of the AGS will rupture and be washed away, thereby affecting the wastewater treatment results.<sup>2</sup>

The composition and content of extracellular polymeric substances (EPS) play important roles in maintaining the stability of AGS.<sup>3</sup> EPS is considered to secrete extracellular macromolecule active substances of floc, biofilm, granular sludge, and other microorganisms, strengthening the microbial structure and promoting cell aggregation by forming a polymer matrix.<sup>4</sup> EPS can be used as an ener-

gy substance for microorganisms in the aerobic starvation stage, but its inner and outer layers have different biological availabilities; the inner layer of EPS can easily be used by microorganisms, while the bioavailability of the outer layer is poor. As a consequence, microorganisms will use the inner layer of EPS as an energy substrate in the starvation stage, forming a different structure between the EPS inner and outer layers, which greatly affects maintenance of the structural stability of granular sludge.<sup>5</sup> Many factors, such as the matrix type and content, as well as operating conditions, among others, affect the EPS content and composition in AGS.<sup>6</sup> In addition, other components of the influent, such as metal ions and phosphorus, will be complexed with various functional groups in EPS, such as the carboxyl group, phosphoric acid, the thiol group, and the phenol and hydroxyl groups, thereby affecting the production of EPS.<sup>7</sup> For example, the presence of cations such as Zn<sup>2+</sup>, Mn<sup>2+</sup>, or Mo<sup>6+</sup> will change the EPS content and composition significantly;<sup>8</sup> the combination of divalent cations with EPS can maintain the microbial aggregate structure.<sup>9</sup>

Phosphorus is an essential nutrient needed for the growth and metabolism of microorganisms.<sup>10</sup> Phosphorus is involved in such activities as the syn-

\*Corresponding author: +86 451-86283028; fax: +86 451-86283028.  
E-mail address: zhonglinchen@hit.edu.cn

thesis of nucleic acids and high-energy compounds adenosine-triphosphate and glucose metabolism in microorganisms. However, many studies on the effect of influent phosphorus concentration on EPS content and composition have mainly focused on the lack of phosphorus content. A phosphorus deficiency may lead to insufficient phosphorus for microbial organisms to synthesize cells, thereby causing metabolic abnormalities that affect microorganism growth; as a result, the proportion of larger granular sludge in the system decreases, influencing AGS stability. A phosphorus deficiency can also induce excessive production of filamentous bacteria, which results in deteriorated sludge settling and bulking of activated sludge,<sup>11</sup> changing the content and composition of EPS.<sup>12</sup> EPS contains a large amount of phosphorus, acting as phosphorus storage or a phosphorus transfer station in the processes of phosphorus release and phosphorus absorption;<sup>13</sup> EPS also participates in the process of biological phosphorus accumulation.<sup>14</sup> Insoluble phosphorus can increase the polysaccharide (PS) content in the EPS of sludge by providing a carrier and inorganic crystal nucleus for microorganisms, which is beneficial to granular sludge formation.<sup>15</sup> EPS containing a large amount of negatively charged phosphorus may affect the electrical charge characteristics of EPS. The use of phosphorus recovery technology and different sources of phosphorus will result in differences in wastewater phosphate content.<sup>16,17</sup> Based on the superiority of AGS, it has been used to treat a variety of wastewater types. However, the effect of influent phosphorus content on the content and composition of sludge EPS and its influence on the properties of EPS in AGS have been rarely mentioned.

EPS can be categorized into loosely bound EPS (LB-EPS) and tightly bound EPS (TB-EPS) according to different distribution positions.<sup>18</sup> TB-EPS is located on the cell body surface and is closely integrated with the cell wall. LB-EPS is distributed outside the TB-EPS, and has loose structure and low density. LB-EPS and TB-EPS have different contents and components, which have different effects on the formation of biological aggregates and the surface properties of granular sludge.<sup>19</sup>

The goal of this study was to evaluate the effect of influent phosphorus concentration on the content, composition, and characteristics of LB-EPS and TB-EPS in long-term AGS by determining the orthophosphate, PS and protein (PN) content, by performing fluorescence spectroscopy, fluorescence region integral (FRI) analysis, and the zeta potential ( $\zeta$ ), in order to provide more detailed information for a stable operation strategy for AGS in different phosphate wastewater treatment processes.

## Materials and methods

### Reactor setup and operation

In this experiment, AGS was cultivated in two identical laboratory-scale sequencing batch reactors (SBR) made of organic glass, each with effective working volumes of 4.20 L. The SBRs were designated as R1 and R2. The SBRs had an internal diameter of 9 cm and height of 85 cm, with the upper part filled with water and the middle part drained, and a volume exchange rate of 50 % in every cycle. The SBRs were run for six 240-min cycles each day. Each cycle consisted of 5 minutes of influent, 210 minutes of aerobic conditions, 5 minutes of settling, 5 minutes of draining, and 15 minutes of idle time. A flow meter was used to control the air flow rate at 1.19 vvm. The dissolved oxygen (DO) concentration was 6.00–8.00 mg L<sup>-1</sup>. The SBRs were operated at room temperature (18–21 °C).

### Sludge and wastewater composition

The inoculated AGS was derived from sludge which was cultured for 60 d at an influent phosphorus concentration of 5.54 to 6.89 mg L<sup>-1</sup> in the R1, and 24.36 to 27.97 mg L<sup>-1</sup> in the R2 reactor; the mixed liquor suspended solids (MLSS) of R1 and R2 were 2317.30 mg L<sup>-1</sup> and 2026.78 mg L<sup>-1</sup>, respectively. The AGS particle size distribution is shown in Fig. 1.

Artificial wastewater was used in this experiment; the compositions of the influent wastewater and the effluent quality are shown in Table 1. Glucose and sodium acetate (2:1) were the carbon sources, ammonium chloride was the nitrogen source, and considering that the phosphate in the sewage was mainly in the form of orthophosphate, phosphorus (total phosphorus) was replaced with

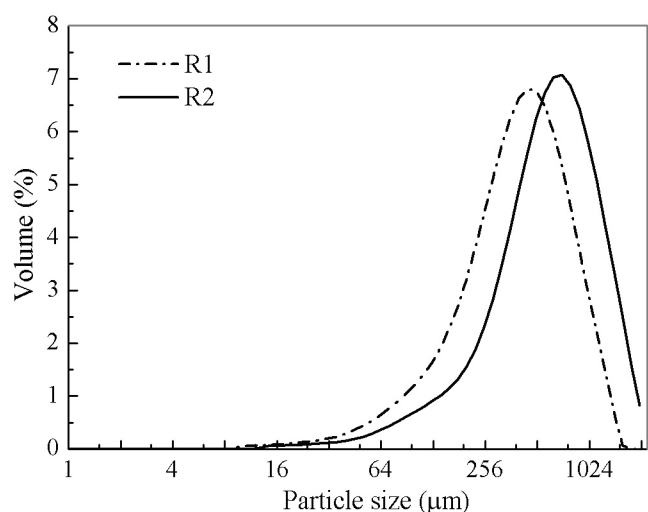


Fig. 1 – AGS particle size distribution in R1 and R2

Table 1 – Characteristics of influent and effluent of AGS reactors R1 and R2

Parameter	Characteristics of influent and effluent			
	influent		effluent	
	R1	R2	R1	R2
PO <sub>4</sub> <sup>3-</sup> -P <sup>a</sup> (mg L <sup>-1</sup> )	5.54–6.89	24.36–27.97	3.60–4.45	20.49–22.61
COD <sup>b</sup> (mg L <sup>-1</sup> )	417.24–538.82		91.18–174.08	88.42–179.61
NH <sub>4</sub> <sup>+</sup> -N <sup>c</sup> (mg L <sup>-1</sup> )	182.06–206.01		0.68–3.82	0.93–8.16
NO <sub>2</sub> <sup>-</sup> -N <sup>d</sup> (mg L <sup>-1</sup> )	0.04–0.07		69.7–93.2	58.7–84.4
NO <sub>3</sub> <sup>-</sup> -N <sup>e</sup> (mg L <sup>-1</sup> )	0–0.02		2.7–4.3	2.2–13.7
pH	7.06–7.88		8.89–9.16	8.62–9.07
CaCl <sub>2</sub> ·2H <sub>2</sub> O (mg L <sup>-1</sup> )	10.00			
MgSO <sub>4</sub> ·7H <sub>2</sub> O (mg L <sup>-1</sup> )	20.00			

orthophosphate;<sup>20</sup> potassium dihydrogen phosphate was the source of phosphorus, and an additional 0.5 mg L<sup>-1</sup> of trace element was added.<sup>21</sup> The pH of the wastewater was stabilized at approximately 7.5 by adding NaHCO<sub>3</sub>.

#### Extraction of LB-EPS and TB-EPS

The sludge mixed liquor samples were collected 5 minutes before the end of aeration. A heat-extraction method was used for TB-EPS extraction and centrifugation was used for LB-EPS. The specific extraction procedures for LB-EPS and TB-EPS can be found in the literature.<sup>21</sup>

#### Analysis of three-dimensional fluorescence spectra, synchronous fluorescence spectroscopy, and fluorescence region integration

The three-dimensional fluorescence spectra (3D-EEM) of the LB-EPS and TB-EPS solutions were identified using a fluorescence spectrophotometer (F-4600, Hitachi, Japan). The range of excitation (EX) wavelength was 220–450 nm increased incrementally by 5 nm, and the scanning emission (EM) spectra from 220 nm to 550 nm were measured in 1 nm increments. The EX and EM slits were maintained at 5 nm, and the scanning speed was 1200 nm min<sup>-1</sup>. The voltage of the photomultiplier tube was maintained at 400 V.

Synchronous scanning fluorescence spectrometry was used to measure the sample with a step value of  $\Delta\lambda = 60$  nm. The range of EX and EM wavelengths were 250–550 nm at 5 nm increments, the scanning speed was adjusted to 240 nm min<sup>-1</sup>, and the EX and EM slits were sited at 5 nm.

FRI was proposed by Chen *et al.*<sup>22</sup> in 2003, and developed on the basis of the traditional peak meth-

od. Chen used FRI to divide the fluorescence spectrum (EEM) into five independent regions for quantitative analysis. The excitation/emission ratio (Ex/Em) of 220–250/280–380 nm was assigned to tyrosine- and tryptophan-like substances, region (I) and region (II), the Ex/Em = 220–250/380–550 nm was identified as the fulvic acid-like region (III), the Ex/Em = 250–450/280–380 nm was identified as the soluble microbial byproduct-like material region (IV), and the Ex/Em >250/ >380 nm was identified as the humic acid-like region (V).

Deionized water was used as a blank during sample analysis. Origin 8.0 software was used for 3D-EEM and synchronous data processing; meanwhile, contour lines were shown for each 3D-EEM spectra to represent the fluorescence intensity. A quantitative analysis of the entire area fluorescence was performed using MATLAB 2016a. The total organic carbon (TOC) content of the solutions was diluted to 10 mg L<sup>-1</sup> before the three-dimensional fluorimetry.

#### Analytical methods

The chemical oxygen demand (COD), ammonium, nitrates, nitrite, orthophosphate, and MLSS of samples were determined by the standard methods.<sup>23</sup> DO was measured with a DO meter (inoLab Oxi 7310, WTW Company, Germany). The PN was measured according to the modified Lowry technique with bovine serum albumin as the standard,<sup>24</sup> and PS was measured using the anthrone-sulfuric acid method with glucose as the standard.<sup>25</sup> The zeta potential of the sample was measured using a zeta potentiometric apparatus (Malvern Zetasizer Nano ZS90, Britain). The TOC was measured using a TOC analyzer (muliN/C2100, Analytikjena, Germany).

## Results and discussion

### Main components of LB-EPS and TB-EPS

PS and PN are generally considered the main components of EPS. The content of PN and PS, and the PN/PS ratio in both LB-EPS and TB-EPS at different influent phosphorus concentrations are illustrated in Fig. 2.

As shown in Fig. 2, the content of PS in LB-EPS decreased from  $8.48 \text{ mg g}^{-1}$  to  $7.15 \text{ mg g}^{-1}$  with the increase in the influent phosphorus concentration, while the content of PN increased from  $2.00 \text{ mg g}^{-1}$  to  $4.64 \text{ mg g}^{-1}$ . LB-EPS had more PS than PN, which was consistent with previous studies.<sup>26</sup> The PS and PN in TB-EPS increased from  $17.75$  and  $64.4 \text{ mg g}^{-1}$  to  $27.68$  and  $137.16 \text{ mg g}^{-1}$ , respectively, which may be sufficient phosphorus to promote microbial metabolism, thereby prompting microorganisms to produce more PS and PN;<sup>27</sup> in addition, EPS contained certain metal ions which can also stimulate microorganisms to produce more PN and PS,<sup>8,21</sup> which work together such that the PN and PS contents increase with increasing influent phosphorus content. TB-EPS contained more PN than PS, and the content of PS and PN in TB-EPS was significantly higher than in LB-EPS, which was aligned with preliminary results.<sup>28</sup> The ratio of PN/PS in LB-EPS and TB-EPS also increased with increasing influent phosphorus concentration. PN plays a crucial role in the structural stability of granular sludge, and the increase in PN in the EPS enhanced the stability of the aerobic granules.<sup>29</sup> In summary, increasing the concentration of influent phosphorus is appropriate for maintaining AGS stability.

### Orthophosphate content in LB-EPS and TB-EPS

Phosphorus exists in a variety of forms, and orthophosphate is the main form of phosphorus in the EPS of AGS;<sup>30</sup> the orthophosphate content of the LB-EPS and the TB-EPS in this experiment is shown in Fig. 3.

As shown in Fig. 3, there were significant impacts on the orthophosphate content of LB-EPS and TB-EPS in the R1 and R2 reactors. The orthophosphate content in LB-EPS increased slightly with the increase in influent phosphorus concentration, only  $0.81 \text{ mg L}^{-1}$ , while the increment of TB-EPS was greater, increasing from  $1.42 \text{ mg g}^{-1}$  to  $3.94 \text{ mg g}^{-1}$ . These results illustrate that the content of orthophosphate in LB-EPS and TB-EPS increases with an increase in influent phosphorus concentration. The increased orthophosphate content of TB-EPS was higher than that of LB-EPS, and the orthophosphate content in TB-EPS accounts for more than 78 % of the total content of orthophosphate in

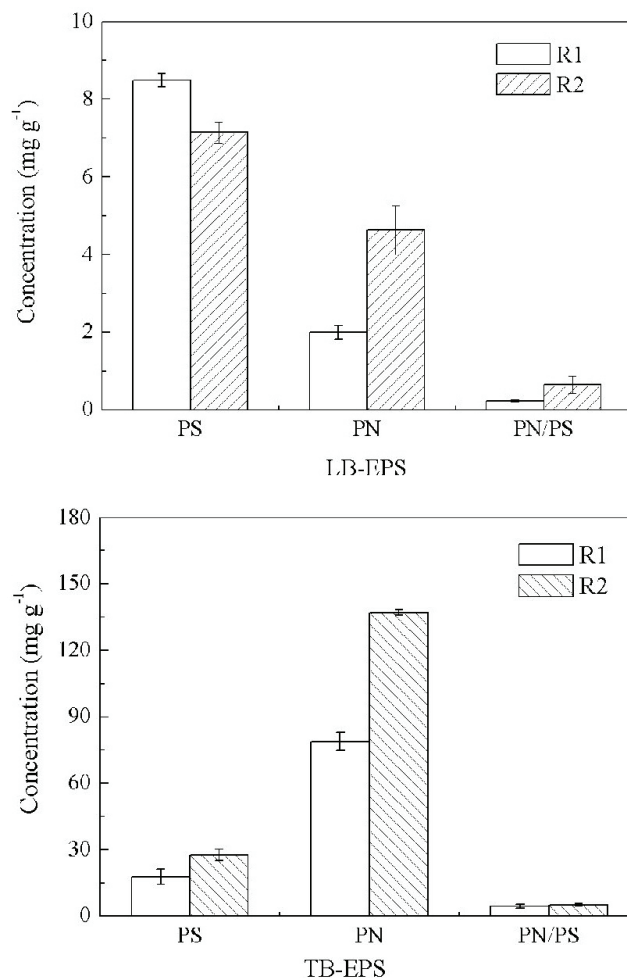


Fig. 2 – PN and PS content and the PN/PS ratio in the LB-EPS and TB-EPS in reactors R1 and R2

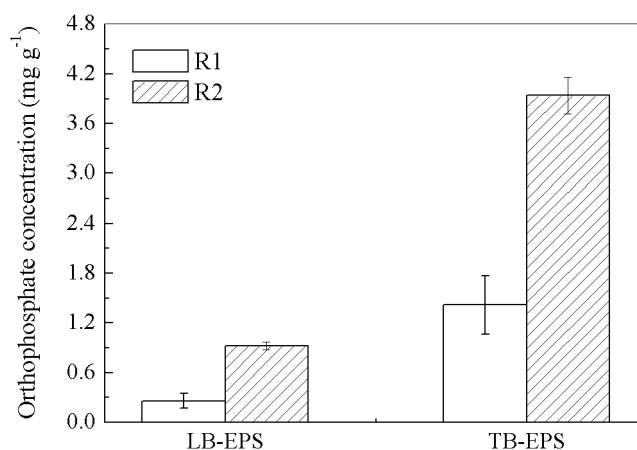


Fig. 3 – Orthophosphate content of LB-EPS and TB-EPS in reactors R1 and R2

each reactor, aligned with previous study results.<sup>14</sup> The reason for this may be because EPS has a certain adsorption and storage function for orthophosphate,<sup>22</sup> in which the LB-EPS only transported and retained orthophosphate, while TB-EPS not only transported and retained orthophosphate but also

participated in biological phosphorus accumulation.<sup>14</sup> Additionally, the EPS extraction method may have influenced the results; different extraction methods can result in different EPS composition and content,<sup>6</sup> affecting the orthophosphate content and distribution.

The previous analysis indicates that TB-EPS plays a larger role than LB-EPS in the processes of orthophosphate adsorption and storage, and that increased influent phosphorus concentration is beneficial for orthophosphate adsorption and storage of LB-EPS and TB-EPS.

### Fluorescence characterization of LB-EPS and TB-EPS

#### 3D-EEM

The 3D-EEM fluorescence spectrum is simple and effective, and it is further employed to characterize the components and structures of LB-EPS and TB-EPS. Fig. 4 shows the 3D-EEM spectra of LB-EPS and TB-EPS with different influent phosphorus concentrations. The fluorescence spectral parameters of LB-EPS and TB-EPS, including the peak locations and fluorescence intensity are sum-

marized in Table 2. There are two main peaks with different fluorescence intensity that can be identified from the LB-EPS and TB-EPS spectra. The first peak was observed at Ex/Em equal to 220–250/320–335 nm (Peak A), which could be attributed to aromatic PN.<sup>22</sup> The second main peak was observed at Ex/Em equal to 275–280/305–340 nm (Peak B), corresponding to tryptophan-like PN.<sup>22</sup> There was also a third peak (Peak C) located at Ex/Em equal to 220–250/380–550 nm, described as a fulvic acid-like fluorescence.<sup>22</sup> The 3D-EEM results revealed the presence of PN and humic acid-like substances in LB-EPS and TB-EPS.

The locations of peak C in the LB-EPS of R1 and R2 were identical, but slightly different for peak A and peak B. R2 compared to R1 has a blueshift of 20 nm in terms of Ex wavelengths, a redshift of 55 nm in terms of Em wavelengths for peak A in LB-EPS. Meanwhile, the location of peak B in TB-EPS of R2 has a blueshift of 2 nm in terms of Em wavelengths; peak A also has a blueshift of 5 nm along the Em axis compared to R1. The shift in the peak position may be due to the decrease in the number of aromatic rings and the decrease in conjugation bonds in the chain structure, or perhaps the

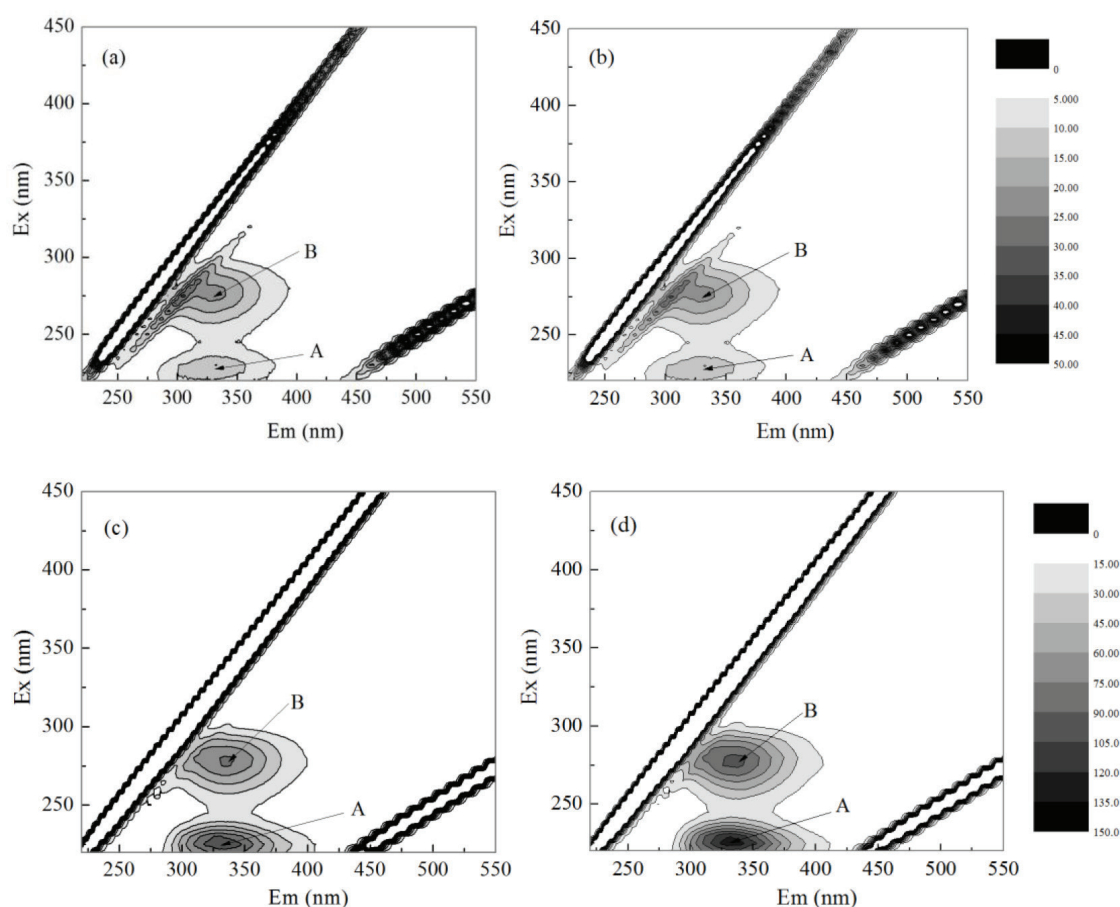


Fig. 4 – 3D-EEM of LB-EPS and TB-EPS in different reactors: (a) LB-EPS of R1, (b) LB-EPS of R2, (c) TB-EPS of R1, (d) TB-EPS of R2

Table 2 – Fluorescence spectral parameters of LB-EPS and TB-EPS in reactors R1 and R2

Sample		Peak A		Peak B		Peak C	
		Ex/Em	Intensity	Ex/Em	Intensity	Ex/Em	Intensity
LB-EPS	R1	250/275	17.02	275/305	32.55	245/535	4.787
	R2	230/330	16.39	275/305	32.11	245/535	4.777
TB-EPS	R1	225/335	102.30	280/336	77.04	230/500	6.325
	R2	225/330	129.40	280/334	94.11	230/500	6.371

presence of the carbonyl-containing substituent, alkoxy, amino groups.<sup>31</sup> These results indicate that the influent phosphorus concentration will influence a chemical structural change in LB-EPS and TB-EPS.

Correspondingly, the fluorescence intensities of the three peaks rarely changed with increased phosphorus concentration in LB-EPS. The peak intensity ranking was peak B > peak A > peak C. However, the fluorescence intensities of peaks A and B increased markedly from 102.3 and 77.04 to 129.4 and 94.11 in TB-EPS, respectively. There was almost no change in the fluorescence intensity and the position of peak C; the peak intensity ranking was peak A > peak B > peak C. Additionally, the peak intensity and the position of the three peaks were obviously different between TB-EPS and LB-EPS; the peak intensity in TB-EPS was higher than that in LB-EPS, except peak C. These results suggest that increased phosphorus concentration had a different effect on LB-EPS and TB-EPS. Aromatic and tryptophan PN-like substances were more important EPS components than was humic acid in maintaining the stability of granular sludge.<sup>32</sup> The results suggest that a high influent phosphorus concentration can promote the production of PN in TB-EPS, which is beneficial to AGS stability.

#### FRI analysis

Fig. 5 shows the percentage distribution of five regional integral standard volumes from FRI analysis of LB-EPS and TB-EPS. The results show that region I and region II accounted for the largest share of relative organic matter in LB-EPS and TB-EPS, accounting for 50.83–60.80 % of EPS; these regions were categorized as PN-likes. This suggests that PN-likes were a major component of EPS, a quantitative result that is consistent with previous 3D-EEM results. Region IV was the second-largest component in LB-EPS, accounting for 16.89 % (R2) and 19.89 % (R1), but Region V was the second-largest component in TB-EPS, accounting for 23.73 % (R1) and 24.88 % (R2). Region III (fulvic acid-like) had the smallest percentage in LB-EPS and TB-EPS. The percentage of fulvic acid-like

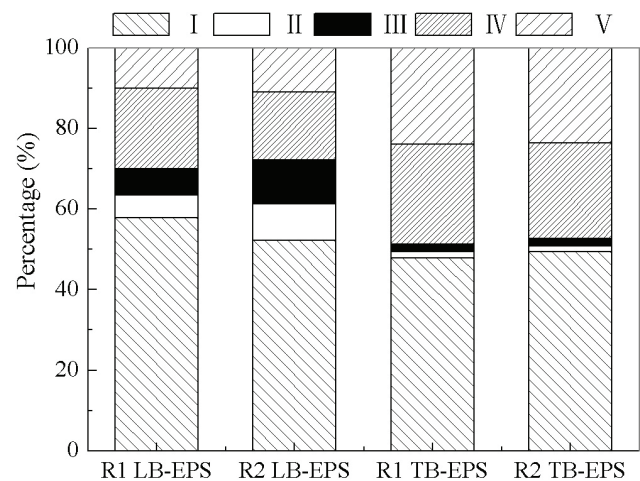


Fig. 5 – Percentage distribution of five regional integral standard volumes of LB-EPS and TB-EPS in R1 and R2

substances in R2 was higher than that in R1 in LB-EPS, while in TB-EPS, the percentage of tyrosine- and tryptophan-like substances was higher. It is possible that the different influent phosphorus concentrations had different effects on LB-EPS and TB-EPS.

As the polymer moves toward the cell center, the relative content of soluble microbial byproduct-likes and humic acid-likes gradually increases, while the content of PN-like substances and fulvic acid-like substances decreases. The main metabolic activity of microorganisms is the decomposition of simple PN-like substances to produce soluble microbial byproduct-likes; high molecular weight and stable humic-like substances are easy to produce in TB-EPS. Clearly, the FRI can provide valuable information to analyze the fluorescence peaks that were not identified with 3D-EEM.

#### Synchronous fluorescence

The synchronous fluorescence spectra of LB-EPS and TB-EPS at different phosphorus concentrations are shown in Fig. 6(a). Based on previous studies,<sup>33</sup> the fluorescence areas corresponding to the wavelength ranges of 250–300, 300–380, and 380–550 nm can be roughly classified as PN-like,

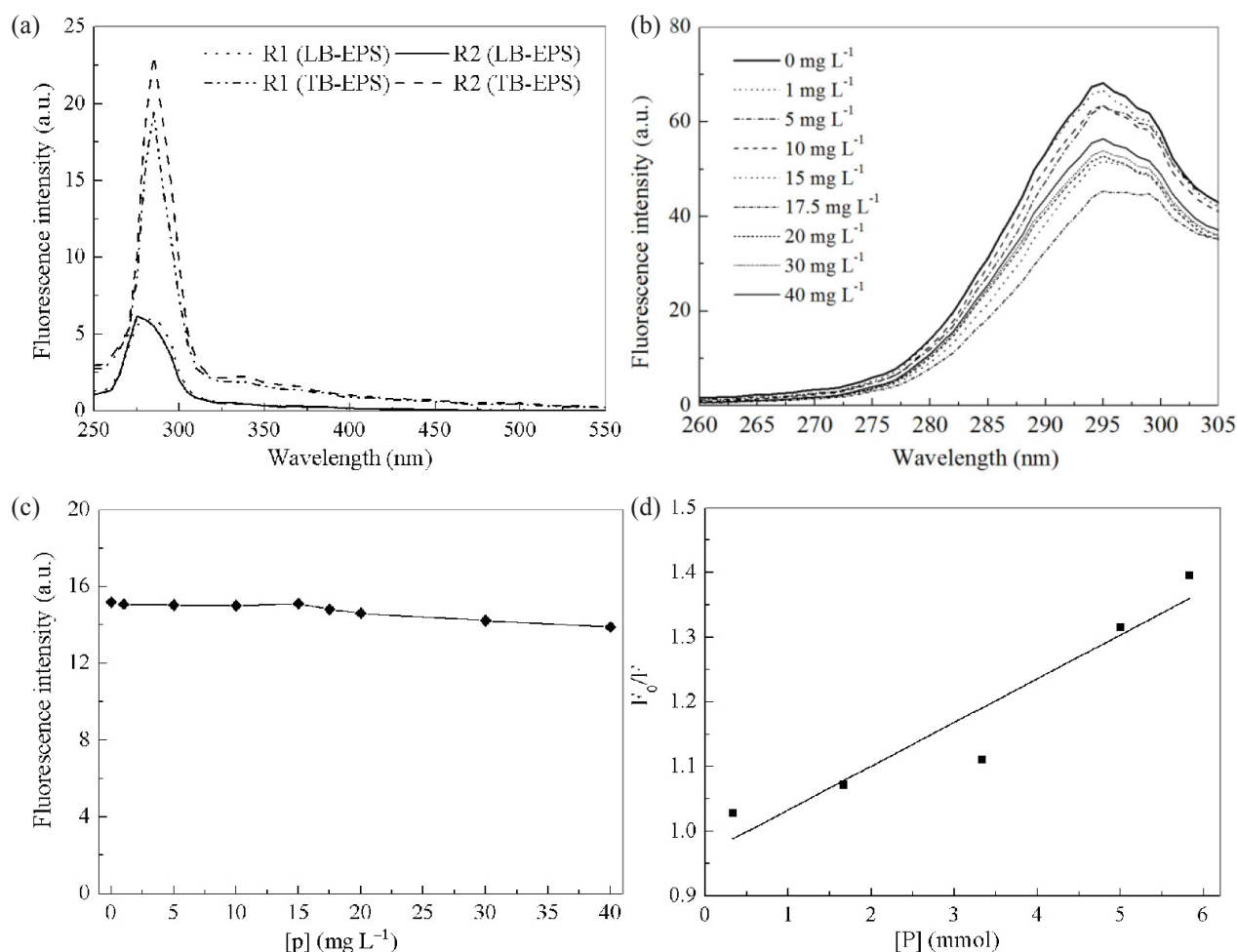


Fig. 6 – Synchronous fluorescence spectra of LB-EPS, TB-EPS in R1 and R2 (a) and EPS (b); Fluorescence intensity of the PN-like substances of EPS (c); Stern-Volmer plot of EPS with increased dosages of P (d)

fulvic-like, and humic-like fluorescence fractions, respectively.

As shown in Fig. 6(a), one obvious fluorescence peak occurred in LB-EPS and TB-EPS, belonging to PN-like substances. The fluorescence intensities of LB-EPS remained almost unchanged with phosphorus concentration (from 6.28 to 6.54 mg L<sup>-1</sup>). At the same time, the fluorescence peak position had a blueshift of 7 nm compared to R1 at the 280 nm fluorescence peak. In TB-EPS, no movement in the fluorescence position occurred, only the intensity of fluorescence increased from 19.58 to 23.45. These results show that the concentration of phosphorus had a greater influence on the fluorescence intensity of TB-EPS compared with that of LB-EPS, higher influent phosphorus concentrations enhanced the production of PN-like substances, which are the main components of LB-EPS and TB-EPS.<sup>33</sup> In addition, other components of EPS, such as phosphorus and metal ions, among others, may also have an impact on EPS fluorescence intensity.

To confirm the influence of phosphorus concentration on the synchronous fluorescence intensi-

ty of EPS, orthophosphate was added to EPS in concentrations of 0, 1, 5, 10, 15, 17.5, 20, 30, and 40 mg L<sup>-1</sup> ( $V_{\text{orthophosphate}}:V_{\text{EPS}} = 1:10$ ), and oscillated at room temperature for 24 h before synchronous fluorometric determination. The peak values of fluorescence intensity with different orthophosphate concentrations are shown in Fig. 6(b). Whether orthophosphate can produce fluorescence quenching to EPS is related to the concentration of influent phosphate and the composition of EPS; the fluorescence intensities slowly decreased from 68.67 to 45.91 while the orthophosphate concentration increased from 0 mg L<sup>-1</sup> to 17.5 mg L<sup>-1</sup>. This indicates that phosphorus content can produce a fluorescence quenching phenomenon in EPS. However, when the orthophosphate concentration increased to 40 mg L<sup>-1</sup>, the fluorescence intensity increased to 56.7, where it had no fluorescence quenching effect on EPS.

Because identical charges repel each other, the negatively charged EPS had difficulty adsorbing the negatively charged phosphorus. However, there were positive charge groups in the EPS, especially

some metal elements that allowed the phosphorus to be contained in the EPS.<sup>21</sup> It is possible that phosphorus interacted with the positive charge groups, such as the metal ions, and then had indirect fluorescence quenching with the organic components of EPS. The phenomenon of indirect quenching will disappear when the concentration of influent phosphate is too high. To investigate whether the fluorescence quenching of EPS on phosphorus had a direct effect, the EPS was extracted by the cation resin method. The same phosphorus concentrations as above were added to the EPS, and synchronous fluorescence was measured after shaking at room temperature for 24 h. As shown in Fig. 6(c), the fluorescence intensity of the PN-like substances did not substantially change, remaining at approximately 14.18. In conclusion, the fluorescence quenching of phosphorus to EPS is mainly the indirect effect of phosphorus on EPS by cations. Further studies are needed in this area.

The mechanism of fluorescence quenching can be divided mainly into dynamic and static quenching based on the interaction between the quencher and the fluorophore.<sup>34</sup> The Stern-Volmer equation can be used to deal with fluorescence quenching data (Eq. (1)):

$$\frac{F_0}{F} = 1 + K_{sv}[Q] = 1 + k_q\tau_0[Q] \quad (1)$$

in which  $F_0$  and  $F$  are the fluorescence intensities with the absence and presence of orthophosphate, respectively.  $K_{sv}$  is the Stern-Volmer quenching rate constant,  $[Q]$  is the concentration of orthophosphate,  $k_q$  is the quenching rate constant of the biological macromolecule, and  $\tau_0$  is the average lifetime of the molecule ( $10^{-8}$  S).

Ordinarily, when the Stern-Volmer model is linear, the quenching is either dynamic or static, and when the model is curvilinear at high concentration, the quenching may be a combination of quenching types.<sup>34</sup> The results showed that  $k_q = 0.67 \cdot 10^{10} < 2.0 \cdot 10^{10}$  L mol<sup>-1</sup> s<sup>-1</sup>, and the Stern-Volmer model was linear, as shown in Fig. 6(d) at orthophosphate concentrations between 0 mg L<sup>-1</sup> and 17.5 mg L<sup>-1</sup>; therefore, the quenching was considered to be dynamic quenching.<sup>34</sup> This finding also indicates that phosphorus can be removed by EPS during wastewater treatment.

### Zeta potential of LB-EPS and TB-EPS

To obtain the surface natures of LB-EPS and TB-EPS, their zeta potential was measured, as shown in Table 3. The zeta potential of LB-EPS and TB-EPS are both negative, because EPS contains more sulfate, phosphate and carboxyl groups (and other negative functional groups), but fewer amino groups and other positive functional groups.<sup>7</sup>

Table 3 – Zeta potential of LB-EPS and TB-EPS in reactors R1 and R2

Sample	Zeta potential (mV)	
	LB-EPS	TB-EPS
R1	-11.15±1.51	-37.35±2.06
R2	-4.97±0.64	-38.85±1.73

Ordinarily, PS is negatively charged while PN is positively charged. In this study, the ratio of PN/PS in R1 (0.23) was less than that in R2 (0.65) in LB-EPS, and although the content of orthophosphate in R2 was slightly higher than that in R1, there were many substances with positive charges, such as metal ions in LB-EPS.<sup>21</sup> The zeta potential of LB-EPS in R1 was lower than that in R2: -11.15 mV and -4.97 mV, respectively. This finding may be the result of the combined action of PN/PS, orthophosphate, and metal ions. However, the zeta potential change in TB-EPS was just the opposite, at -37.35 mV and -38.85 mV, respectively. When the ratio of PN/PS in R1 (4.45) and R2 (4.95) was similar, it was mainly because the orthophosphate content in R2 was considerably higher than that of R1 in TB-EPS, which was more than 2.52 mg g<sup>-1</sup>. However, further studies are needed to explain why the zeta potential of LB-EPS and TB-EPS varied with influent phosphorus concentration.

The zeta potential in TB-EPS was significantly lower than that in LB-EPS, which was consistent with previous studies.<sup>35</sup> The zeta potential of AGS was significantly lower than that of floc sludge; the zeta potential of LB-EPS can reflect the electrochemical properties of sludge better than that of TB-EPS, and plays a major role in the formation and stability of aerobic granules.<sup>35</sup> Therefore, it may be concluded that a higher influent phosphorus concentration is appropriate for AGS formation and stability.

### Conclusions

The influent phosphorus concentration affects the content, orthophosphate content, zeta potential, and fluorescence characterizations of LB-EPS and TB-EPS. The phosphorus, PN and PS content in LB-EPS and TB-EPS were higher when the influent phosphorus concentration increased, except for PS in LB-EPS. With higher influent phosphorus concentration, the zeta potential of LB-EPS was lower, while for TB-EPS, the result was opposite. Whether phosphorus can produce fluorescence quenching to EPS is related to the influent phosphorus concentration and the composition of EPS. The PN-like substances are the major component of EPS, and higher



phosphorus caused the TB-EPS to contain large amounts of PN-like substances, while it did not change considerably in LB-EPS. The PN was the key component in AGS stability.

### ACKNOWLEDGMENTS

*This work was supported by The National Key Technology R&D Program (2018YFD0800105); National Natural Science Foundation of China (NO. 51208084); Open Project of State Key Laboratory of Urban Water Resource and Environment, Harbin Institute of Technology (No. QA201819).*

### References

- Dilaconi, C., Ramadori, R., Lopez, A., Hydraulic shear stress calculation in a sequencing batch biofilm reactor with granular biomass, *J. Environ. Sci. Technol.* **39** (2005) 889. doi: <https://doi.org/10.1021/es0400483>
- Pijuan, M., Werner, U., Yuan, Z., Reducing the start up time of aerobic granular sludge reactors through seeding floccular sludge with crushed aerobic granules, *Water Res.* **45** (2011) 5075. doi: <https://doi.org/10.1016/j.watres.2011.07.009>
- Mcswain, B. S., Irvine, R. L., Hausner, M., Composition and distribution of extracellular polymeric substances in aerobic flocs and granular sludge, *J. Appl. Environ. Microb.* **71** (2005) 1051. doi: <https://doi.org/10.1128/AEM.71.2.1051-1057.2005>
- Tay, J. H., Liu, Q. S., Liu, Y., The role of cellular polysaccharides in the formation and stability of aerobic granules, *J. Lett. Appl. Microbiol.* **33** (2001) 222. doi: <https://doi.org/10.1046/j.1472-765x.2001.00986.x>
- Wang, Z. W., Liu, Y., Tay, J. H., Distribution of EPS and cell surface hydrophobicity in aerobic granules, *J. Appl. Environ. Microb.* **69** (2005) 469. doi: <https://doi.org/10.1007/s00253-005-1991-5>
- Sheng, G. P., Yu, H. Q., Li, X. Y., Extracellular polymeric substances (EPS) of microbial aggregates in biological wastewater treatment systems, *J. Biotechnol. Adv.* **28** (2010) 882. doi: <https://doi.org/10.1016/j.biotechadv.2010.08.001>
- Liu, H., Fang, H. H. P., Characterization of electrostatic binding sites of extracellular polymers by linear programming analysis of titration data, *J. Biotechnol. Bioeng.* **80** (2002) 806. doi: <https://doi.org/10.1002/bit.10432>
- Cao, X. S., Long, T. R., Meng, X. Z., Effects of Mn<sup>2+</sup>, Mo<sup>6+</sup> and Zn<sup>2+</sup> on the components change of extracellular polymeric substances in activated sludge, *J. Environ. Sci.-China* **25** (2004) 71.
- Mayer, C., Moritz, R., Kirschner, C., Borchard, W., The role of intermolecular interactions: studies on model systems for bacterial biofilms, *Int. J. Biol. Macromol.* **26** (1999) 3. doi: [https://doi.org/10.1016/S0141-8130\(99\)00057-4](https://doi.org/10.1016/S0141-8130(99)00057-4)
- Zevin, A. S., Nam, T., Rittmann, B., Krajmalnik-Brown, R., Effects of phosphate limitation on soluble microbial products and microbial community structure in semi-continuous Synechocystis-based photobioreactors, *Biotechnol. Bioeng.* **112** (2015) 1761. doi: <https://doi.org/10.1002/bit.25602>
- Guo, J. H., Peng, Y. Z., Wang, S. Y., Filamentous and non-filamentous bulking of activated sludge encountered under nutrients limitation or deficiency conditions, *Chem. Eng. J.* **255** (2014) 453. doi: <https://doi.org/10.1016/j.cej.2014.06.075>
- Hoa, P. T., Nair, L., Visvanathan, C., The effect of nutrients on extracellular polymeric substances production and its influence on sludge properties, *Water SA.* **29** (2003) 437.
- Zhang, H. L., Wei, F., Wang, Y. P., Phosphorus removal in an enhanced biological phosphorus removal process: Roles of extracellular polymeric substances, *J. Environ. Sci. Technol.* **47** (2013) 11482. doi: <https://doi.org/10.1021/es403227p>
- Long, X., Tang, R., Fang, Z., Xie, C., Li, Y., Xian, G., The roles of loosely-bound and tightly-bound extracellular polymer substances in enhanced biological phosphorus removal, *Chemosphere* **189** (2017) 679. doi: <https://doi.org/10.1016/j.chemosphere.2017.09.067>
- Wang, G. W., Wang, D., Xu, X. C., Partial nitrifying granule stimulated by struvite carrier in treating pharmaceutical wastewater, *Appl. Microbiol. Biot.* **97** (2013) 8757. doi: <https://doi.org/10.1007/s00253-012-4546-6>
- Ma, H. Y., Zhang, Y. L., Xue, Y., Li, Y. Y., A new process for simultaneous nitrogen removal and phosphorus recovery using an anammox expanded bed reactor, *Bioresour. Technol.* **267** (2018) 201. doi: <https://doi.org/10.1016/j.biortech.2018.07.044>
- Quist-Jensen, C. A., Sørensen, J. M., Svenstrup, A., Scarpa, L., Carlsen, T. S., Jensen, H. C., Wýbrandt, L., Christensen, M. L., Membrane crystallization for phosphorus recovery and ammonia stripping from reject water from sludge dewatering process, *Desalination* **440** (2018) 156. doi: <https://doi.org/10.1016/j.desal.2017.11.034>
- Han, X. M., Wang, Z. W., Zhu, C. W., Wu, Z. C., Effect of ultrasonic power density on extracting loosely bound and tightly bound extracellular polymeric substances, *Desalination* **329** (2013) 35. doi: <https://doi.org/10.1016/j.desal.2013.09.002>
- Bezawada, J., Hoang, N. V., More, T. T., Production of extracellular polymeric substances (EPS) by using wastewater sludge as raw material and flocculation activity of the EPS produced, *J. Environ. Manage.* **128** (2013) 83. doi: <https://doi.org/10.1016/j.jenvman.2013.04.039>
- Ge, J., Meng, X. G., Song, Y. H., Terracciano, A., Effect of phosphate releasing in activated sludge on phosphorus removal from municipal wastewater, *J. Environ. Sci.* **67** (2018) 216. doi: <https://doi.org/10.1016/j.jes.2017.09.004>
- Yan, L. L., Liu, Y., Wen, Y., Ren, Y., Hao, G. X., Zhang, Y., Role and significance of extracellular polymeric substances from granular sludge for simultaneous removal of organic matter and ammonia nitrogen, *Bioresour. Technol.* **179** (2015) 460. doi: <https://doi.org/10.1016/j.biortech.2014.12.042>
- Chen, W., Westerhoff, P., Leenheer, J. A., Booksh, K., Fluorescence excitation-emission matrix regional integration to quantify spectra for dissolved organic matter, *Environ. Sci. Technol.* **37** (2003) 5701. doi: <https://doi.org/10.1021/es034354c>
- APHA, Standard Methods for the Examination of Water and Wastewater. American Public Health Association. Washington DC (1998).
- Lowry, O. H., Rosebrough, N. J., Lewis Farr, A., Randall, R. J., Protein measurement with the folin phenol reagent, *J. Biol. Chem.* **193** (1951) 265.

25. Frølund, B., Palmgren, R., Keiding, K., Nielsen, P. H., Extraction of extracellular polymers from activated sludge using a cation exchange resin, *Water Res.* **30** (1996) 1749. doi: [https://doi.org/10.1016/0043-1354\(95\)00323-1](https://doi.org/10.1016/0043-1354(95)00323-1)
26. Basuvaraj, M., Fein, J., Liss, S. N., Protein and polysaccharide content of tightly and loosely bound extracellular polymeric substances and the development of a granular activated sludge floc, *J. Water Res.* **82** (2015) 104. doi: <https://doi.org/10.1016/j.watres.2015.05.014>
27. Zhou, Y., Nguyen, B. T., Zhou, C., Straka, L., Lai, Y. S., Xia, S., The distribution of phosphorus and its transformations during batch growth of *Synechocystis*, *Water Res.* **122** (2017) 355. doi: <https://doi.org/10.1016/j.watres.2017.06.017>
28. Yan, L. L., Zhang, X. L., Hao, G. X., Guo, Y. H., Ren, Y., Yu, L. B., Bao, X. F., Zhang, Y., Insight into the roles of tightly and loosely bound extracellular polymeric substances on a granular sludge in ammonium nitrogen removal, *Bioresource Technol.* **222** (2016) 408. doi: <https://doi.org/10.1016/j.biortech.2016.10.011>
29. Yu, G. H., He, P. J., Shao, L. M., Lee, D. J., Mujumdar, A. S., Extracellular polymeric substances (EPS) and extracellular enzymes in aerobic granules, *Dry. Technol.* **28** (2010) 910. doi: <https://doi.org/10.1080/07373937.2010.490766>
30. Zhang, Z. C., Huang, X., Study on enhanced biological phosphorus removal using membrane bioreactor at different sludge retention times, *J. Environ. Pollut.* **45** (2011) 15. doi: <https://doi.org/10.1504/IJEP.2011.039081>
31. Wietlik, J. S., Dabrowska, A., Raczek-Stanislawiak, U., Nawrocki, J., Reactivity of natural organic matter fractions with chloride dioxide and ozone, *Water Res.* **38** (2004) 547. doi: <https://doi.org/10.1016/j.watres.2003.10.034>
32. Zhu, L., Qi, H. Y., Lv, M. L., Kong, Y., Yu, Y. W., Xu, X. Y., Component analysis of extracellular polymeric substances (EPS) during aerobic sludge granulation using FTIR and 3D-EEM technologies, *Bioresource Technol.* **124** (2012) 455. doi: <https://doi.org/10.1016/j.biortech.2012.08.059>
33. Chen, W., Habibul, N., Liu, X. Y., Sheng, G. P., Yu, H. Q., FTIR and synchronous fluorescence heterospectral two-dimensional correlation analyses on the binding characteristics of copper onto dissolved organic matter, *Environ. Sci. Technol.* **49** (2015) 2052. doi: <https://doi.org/10.1021/es5049495>
34. Li, N., Wei, D., Wang, S., Comparative study of the role of extracellular polymeric substances in biosorption of Ni(II) onto aerobic/anaerobic granular sludge, *J. Colloid. Interf. Sci.* **490** (2017) 754. doi: <https://doi.org/10.1016/j.jcis.2016.12.006>
35. Su, B. S., Qu, Z., Song, Y. H., Investigation of measurement methods and characterization of zeta potential for aerobic granular sludge, *J. Environ. Chem. Eng.* **2** (2014) 1142. doi: <https://doi.org/10.1016/j.jece.2014.03.006>